TIMBOU-AFRICA PUBLICATION INTERNATIONAL JOURNAL MAY, 2025 EDITIONS.

INTERNATIONAL JOURNAL OF ENGINEERING RESEARCH AND TECHNOLOGY
VOL. 8 NO. 5 E-ISSN 3027-1770 P-ISSN 3026-8095

EVALUATION AND ADSORPTION MODELING OF CONTINUOUS ADSORPTION OF MALACHITE GREEN PIGMENTS ONTO SAWDUST-DERIVED ACTIVATED CARBON IN A FIXED BED COLUMN

AKAKABOTA A. O.; OHIMOR E. O.; & ISIAKPERE PRECIOUS

Department of Chemical Engineering, Federal University of Petroleum Resources, Effurun, Nigeria

Corresponding Author:

akakabota.ambrose@fupr.edu.ng

DOI: https://doi.org/10.70382/tijert.v08i5.011

ABSTRACT

The study was conducted to investigate the adsorption of malachite green dye onto activated carbon prepared from sawdust in a fixed-bed column, with the aim of understanding the process dynamics and improving pollutant removal efficiency. The prepared activated carbon was characterized by Scanning Electron Microscopy with Energy Dispersive X-ray Spectroscopy (SEM-EDS), Fourier Transform Infrared Spectroscopy

INTRODUCTION

Malachite Green is a dangerous artificial dye, which is extremely dangerous for aquatic life, human health, and the environment. It is poisonous and linked to the risk of cancer in vital organs like the heart, kidneys, and breasts. According to Jabar et al. (2023), it disturbs the ecological stability of aquatic habitats. malachite green is a common industrial dye and organic contaminant that is frequently found in wastewater (Oladoye et al. 2023). Due to the health risks it is associated with, the removal of Malachite Green from wastewater is very crucial.

Among the various methods developed for wastewater treatment, adsorption stands out as one of the most effective and versatile techniques due to its simplicity, efficiency, and ability to remove a wide range of pollutants (Satyam and Patra, 2024).

(FTIR), and Brunauer-Emmett-Teller (BET) surface area analysis. The column performances were evaluated by varying bed heights (1.25, 2.5, and 5.0 cm) while keeping other factors such as influent flow rate (5 ml/min) and concentration (500 mg/L) constant to obtain experimental breakthrough curves. From the breakthrough curves, it was observed that the breakthrough time, tb, increased from 180 mins to 270 and 330 mins for bed heights of 1.25, 2.5, and 5 cm, respectively. The exhaustion time (td) for the adsorbent bed was found to increase from 390 mins to 420 mins and 510 mins as bed height increased from 1.25 to 2.5 and 5 cm, respectively. The adsorption capacity, q0, was found to be 221.54, 148.34, and 91.22 mg/g for bed heights of 1.25, 2.5, and 5 cm, respectively. The removal efficiency of malachite green was found to be 54.53%, 67%, and 68.82% for bed heights of 1.25, 2.5, and 5 cm, respectively. The performance of the column was analyzed using the Thomas, Adams-Bohart, and Yoon-Nelson models. The rate constant for all three models decreased with increasing bed heights, while the time required for 50% adsorbate breakthrough increased with increasing bed height. The Adams-Bohart model, which presented consistently high R^2 values within the range of 0.8344 to 0.9229, is the most suitable model for describing the experimental data.

Keywords: Malachite green, Fixed bed, Adsorption, Saw dust, Activated carbon

The use of adsorption in wastewater treatment dates back to the late 19th century, with R. V. Ostrejko's 1900 patent for the first activated carbon filter representing a major achievement (Majji *et al.,* 2021). Since then, activated carbon has been widely used as an adsorbent in water purification due to its high surface area, porosity, and strong affinity for organic compounds.

In the adsorption process, materials tend to concentrate at the surface or interface between two phases, a phenomenon known as interphase accumulation. The material that is adsorbed onto the surface of another substance is referred to as the adsorbate, while the bulk substance on which the adsorption occurs is called the adsorbent.

In view of the severe health and environmental hazards posed by malachite green dye, its effective removal from wastewater remains an urgent priority (Oladoye et al., 2023). While adsorption is widely recognized as an efficient and versatile method for dye removal, there is a paucity of research focusing on low-cost, sustainable adsorbents in fixed-bed column systems, particularly those derived from abundant biomass wastes such as sawdust.

Most prior studies have emphasized batch adsorption systems, leaving a gap in understanding the dynamic behavior, breakthrough characteristics, and kinetic modeling of malachite green adsorption in continuous flow operations. This study addresses these gaps by developing activated carbon from sawdust, characterizing it using SEM-EDS, FTIR, and BET analyses, and systematically evaluating its fixed-bed column performance under varying bed heights.

With liquid-solid adsorption being the most commonly employed in water and wastewater treatment (Patel, 2019), the novelty lies in coupling waste-to-resource valorization with fixed-bed adsorption modeling to optimize dye removal efficiency, providing both an environmentally friendly and economically viable treatment approach. The aim is to enhance pollutant removal efficiency through a deeper understanding of adsorption dynamics, ultimately contributing to safer wastewater management and environmental protection.

LITERATURE REVIEW

Industrial wastewater

Industrial wastewater is water that has been contaminated during various industrial processes. It often contains a variety of pollutants, including heavy metals, toxic chemicals, organic compounds, and suspended solids, which can be harmful to the environment and human health if not properly treated before being released into water bodies. Separation of organic pollutants from wastewaters is imperative before discharging industrial wastewaters into marine environment (Award et al., 2019).

Textile waste water

The textile industry is a major source of industrial wastewater, primarily due to its use of large quantities of water and chemicals throughout various stages of fabric production and processing. The effluent released from textile manufacturing processes can have a significant impact on water quality if not treated properly before discharge. The textile industry is known to consume 1000 of the 100,000 types of dyes present in the commercial market. The annual production rate of dyes is estimated to be about 700,000 tons (Samarghandi et al., 2020).

Textile dyes

Dyes are colouring and valuable compounds for industrial products, particularly in textile industries to dye textiles, yarns, plastics, and other substrates (Fito et al., 2023). These dyes are often non-biodegradable and can be toxic to aquatic life, leading to water pollution and discolouration in water bodies. Common dyes

E-ISSN 3027-1770
P-ISSN 3026-8095

include malachite green, methylene blue, and indigo dyes, each of which can pose environmental challenges.

Textile dyeing is one of the most water-intensive processes, where different types of synthetic dyes (e.g., azo dyes, reactive dyes) are used to colour fabrics. Various synthetic dyes and pigments are ordinarily utilised in the textile-processing industry. Therefore, there is a definite requirement for effluent treatment that is cost-effective to reduce colour substances and auxiliaries from wastewater (Jadhav and Jadhav, 2021).

Waste water treatment

Wastewater treatment is the process of removing contaminants and pollutants from wastewater, ensuring the protection of human health, environmental sustainability, and water resources. The pollution of water bodies by heavy metal effluents from numerous industrial activities is a major environmental challenge that disrupts the ecosystem (Dim et al., 2021). There are three major processes of wastewater treatment. These processes include primary treatment, secondary treatment and tertiary treatment such as filtration and adsorption.

Adsorption

The adsorption technique is the simplest method used for the decontamination of heavy metals in discharged effluents (Dim et al., 2021). Adsorption is one of the technologies used in tertiary treatment to remove dissolved solids and organics, reduce colour, odour, and taste, to eliminate specific pollutants (e.g., heavy metals, pesticides), to remove micro-pollutants (e.g., pharmaceuticals, personal care products), to enhance nutrient removal (e.g., phosphorus, nitrogen), and to improve effluent quality for reuse or discharge.

The principles of adsorption revolve around several key concepts, starting with equilibrium, which is the balance formed between the adsorbent and the adsorbate and is often described by isotherms like Langmuir, Freundlich, and BET. This equilibrium, however, is influenced by adsorption kinetics, which are shaped by factors such as surface area, diffusion, and concentration. Together, these isotherms provide mathematical models to define and understand adsorption equilibrium.

The adsorption performance of an adsorbent is influenced by its chemical and physical structures. While the chemical structure particularly the functional groups, dictates the nature of the adsorption forces present in the adsorbent, the physical structure which includes factors like specific surface area and pore size, affects the accessibility of the adsorbent for dyes (Li et al., 2019).

Several factors influence the adsorption process. The pH level affects the surface charge and the chemistry of the adsorbate, while the concentration of the adsorbate impacts both the kinetics of adsorption and the equilibrium state. Additionally, an increased surface area enhances the adsorption capacity, and the particle size can affect the diffusion rate and overall adsorption kinetics.

However, while various methods have been proposed for dye removal, adsorption processes remain the most appealing due to their simplicity and cost-effectiveness (Li et al., 2019).

In contrast to removal methods such as chemical precipitation, adsorption selectively targets specific contaminants often at a lower cost, while chemical precipitation typically requires the addition of chemicals and pH control, making it more complex.

Furthermore, when compared to biological treatment, adsorption is particularly effective for toxic or non-biodegradable compounds, whereas biological methods excel at removing biodegradable organics, generally requiring longer retention times.

Although Adsorption offers a range of advantages, including high efficiency, low cost, flexibility, and ease of operation, it also has limitations. These limitations include the saturation of the adsorbent capacity, which necessitates regeneration to maintain effectiveness, and the issue of competitive adsorption, where multiple contaminants compete for the same adsorption sites.

Activated carbon adsorption

Activated carbon is a highly porous material derived from organic sources (e.g., sawdust, coconut shells, bamboo, coal). Its surface area is greatly increased through thermal or chemical activation, creating millions of tiny pores that attract and trap contaminants.

Activated carbon, made from natural materials, has been crucial for cleaning water since the early 20th century because it can remove numerous types of pollutants (Satyam and Patra, 2024). It offers several significant advantages that make it a preferred choice for various applications in contaminant removal.

One of the most notable benefits of activated carbon, is its high efficiency, as it is capable of effectively removing a wide range of contaminants, including volatile organic compounds, heavy metals, and other harmful substances.

Many locally prepared activated carbons have been produced and used for the removal of various pollutants from industrial wastewater (Fito et al., 2023). It is relatively low-cost when compared to other advanced treatment technologies, making it a more accessible option for many users. It can also be employed in

E-ISSN 3027-1770
P-ISSN 3026-8095

various treatment configurations, including fixed beds, batch processes, and fluidised beds, allowing for flexible integration into existing systems.

One of the primary mechanisms at play in adsorption is physical attraction which occurs through Van der Waals forces. These are weak, intermolecular forces that enable contaminants to be attracted to the activated carbon surface. This form of adsorption is largely dependent on the proximity of the contaminants to the carbon, allowing for a broad range of substances to be effectively captured.

In the physical adsorption method, pollutants from the wastewater get accumulated on the surface of the adsorbent by the interaction with the physical forces. This is even though chemical adsorption is definite when the adsorbate is chemically attached to the surface of the adsorbent, which is because of the interchange of electrons (Jadhav and Jadhav, 2021).

In addition to physical attraction, adsorption can also be driven by chemical reactions, which involve more robust interactions. Electrostatic interactions play a critical role in this process, as charged contaminants may be attracted to oppositely charged sites on the carbon surface, leading to stronger binding.

As a result of the aforementioned, chemical bonding can occur, wherein specific functional groups on the carbon surface form covalent or ionic bonds with the contaminants. This type of adsorption generally results in a higher degree of retention and removal efficiency.

The adsorption capacity of the synthetic dyes onto activated carbon usually depends on the superficial charge present on the adsorbent when it is in contact with water. Usually, the superficial charge of the carbon will be neutral, and therefore it will dominate the physical adsorption (Jadhav and Jadhav, 2021).

Another important mechanism contributing to the overall adsorption process is size exclusion. Activated carbon possesses a porous structure, and the size of these pores can act as a filter, effectively trapping larger contaminants while allowing smaller molecules to pass through. This selective filtering capacity enhances the efficiency of activated carbon as an adsorbent by ensuring that it can preferentially capture and retain a variety of contaminants, thereby maximising its effectiveness in various treatment applications.

Sawdust-activated carbon

Adsorbents can be sourced from a variety of agricultural wastes and industrial byproducts, including ashes, sawdust, lignin, sunflower shells, corn cobs, clays, and activated carbon (Jadhav and Jadhav, 2021). Among these, sawdust, which happens to be a common byproduct of the wood industry, holds particular promise. When processed into activated carbon, it offers a sustainable, low-cost

option for water treatment and other uses. The activation process can be carried out using thermal, chemical, or physical methods, each enhancing its adsorption capacity in different ways.

Malachite green adsorption on activated carbon

Water pollution poses a serious threat to the sustainability of life on Earth. Among its many causes, the uncontrolled discharge of synthetic dyes into water bodies without adequate treatment remains a major concern (Ahmad et al., 2021).

Due to the ineffectiveness of conventional wastewater treatment techniques for decontamination of persistent and toxic pollutants like malachite green dye, The characteristics of activated carbon make it highly effective in trapping and holding malachite green molecules, thus facilitating efficient adsorption processes.

Several factors influence the adsorption of malachite green onto activated carbon. The pH level plays a significant role, with the optimal range being between 4 and 7 for maximum adsorption efficiency. Temperature also affects the process, as higher temperatures tend to reduce the adsorption capacity. Similarly, higher malachite green concentrations can lead to decreased adsorption efficiency, while an increase in the surface area of activated carbon can enhance its adsorption capacity.

Material degradability

Material degradation and stability depend on various factors, such as the characteristics of the adsorbent (e.g., chemical composition, crystallinity, morphology), the properties of the adsorbate (e.g., acidity, redox potential, biodegradability), and the operating conditions such as, temperature, pH, contact time (Crini and Lichtfouse, 2019).

One of the current limitations of adsorption techniques is that the material degradation and stability of most adsorbents are still relatively low compared to the harsh and complex conditions of wastewater (Satyam and Patra, 2024).

In a study by Chopra and Sondhi, 2022, there was increase in rate of degradation of malachite green with the increase of pH. However, the maximum degradation rate of 99.31±0.97% was observed at pH 8, with further increase in pH, leading to decreased rate of decolourisation and the observance of a downward curve.

The maximum degradation of malachite green dye was observed at 50°C which observed to 92.95±1.65% with further increase in temperature the rate of decolourisation decreased and a downward curve was observed.

Adsorption isotherms

Adsorption isotherm models can describe the interaction mechanisms between the adsorbent and the adsorbate at a constant temperature by analysing the equilibrium data and the properties of both substances (Mohammad et al., 2020). These models are typically established when the adsorbate and adsorbent have had sufficient contact time, allowing the concentration at the interface to reach dynamic equilibrium with the adsorbate concentration in the bulk solution.

Several isotherm models have been applied to adsorption systems, including the Langmuir model, the linear model, the Freundlich model, the Sips model, the Temkin model, and the Brunauer-Emmett-Teller (BET) model (Wang and Guo, 2020). They are primarily equilibrium models that describe how adsorbates interact with adsorbents at the surface level in batch systems.

The isotherm model is represented by a curve that depicts the relationship between the amount of adsorbate onto the adsorbent and concentration (if liquid) or pressure (if gas) at constant temperature. The several types of established isotherms are based on being fitted to different assumptions and cases (Abdelrahman and Shifa, 2019).

With this regard, the interaction is said to be monolayer if the data fits well to the langmuir isotherm and multilayer if the data fit is inclined to the freundlich model (Mengistu et al., 2023). Moreover, the surface interaction is heterogeneous if the data is well represented by freundlich and homogenous if the langmuir model is found to be explanatory. On the other hand, temkin isotherm gives a clue to heat transfer during adsorption.

Langmuir adsorption isotherm

Assumes monolayer adsorption, where adsorbate molecules occupy a fixed number of sites. According to Hashim et al., 2021, it can be expressed as;

$$Ceq/qe=. 1/qmaxCeq + 1/bqmax \quad (2.1)$$

Where: qe represents the quantity of the substance adsorbed at equilibrium per unit mass of the adsorbent.

qmax denotes the maximum adsorption capacity corresponding to monolayer coverage,

Ceq is the equilibrium concentration of the substance.

b is the Langmuir equilibrium adsorption constant.

Freundlich adsorption isotherm

This isotherm describes multilayer adsorption, where adsorbate molecules interact with each other. The Freundlich isotherm model indicates that the ratio of

the adsorbate adsorbed onto a given mass of adsorbent varies with different concentrations of the solution, meaning it is not constant. Unlike models restricted to monolayer adsorption, the Freundlich model can describe multilayer adsorption. According to Hashim et al., 2021, the Freundlich isotherm is expressed as:

$$\ln qe = \ln Kf + 1/n \ln Ce \quad (2.2)$$

$$qe = Kf\, Ce^{1/n}$$

Where:

qe: Sorbate concentration in the solid phase at equilibrium (mg/g)

Ce: Sorbate concentration in the solution at equilibrium (mg/L)

Kf: Freundlich isotherm constant related to adsorption capacity (L/mg)

n: Freundlich exponent, related to adsorption intensity

A linear plot of qe versus log Ce allows for the determination of n and Kf which can be obtained from the slope and the intercept. The value of 1/n indicates the nature of the isotherm: it is irreversible when 1/n = 0, favorable when ($0 < 1/n < 1$), and unfavorable when $1/n > 1$.

El-Awardy adsorption isotherm

This isotherm model describes the adsorption behavior of a solute onto an adsorbent in a fixed bed column. According to Duduna et al., 2019, the El-Awardy isotherm equation is expressed as:

$$\log \theta / (1 - \theta) = \log K + y \log C \quad (2.3)$$

Where;

θ: Fractional surface coverage (dimensionless)

K: Equilibrium constant (L/mg)

C: Concentration of malachite green (mg/L)

y: Heterogeneity factor (dimensionless), possibly indicating the number of molecules interacting with each active site during the adsorption process.

4. Temkin adsorption isotherm: This model combines langmuir and freundlich models. It is effective for describing the adsorption of molecules onto a surface, particularly in systems where interactions between the adsorbate and adsorbent are significant.

According to Hashim et al., 2021, it can be expressed as:

$$qe = RT/bT \ln At + RT/bT \ln Ce \quad (2.4)$$

Where;

$\beta = RT/bT$

qe represents the quantity of adsorbate that is adsorbed per unit mass of the adsorbent at equilibrium.

Ce is the concentration of the adsorbate at equilibrium.
bT is the Temkin equilibrium adsorption constant
β is a Temkin isotherm constant associated with the equilibrium binding constant, which reflects the maximum binding capacity.
At is another Temkin isotherm constant related to the heat of adsorption.
T is the absolute temperature (in Kelvin), and R is the universal gas constant, valued at 8.314 J/mol·K. The constant b represents the Temkin parameter related to the heat of sorption (J/mg).

Fixed bed column for adsorption

A fixed bed column typically consists of a column, which is a cylindrical vessel filled with adsorbent material. It consists of adsorbent, a granular or powdered material with high surface area. There's also an inlet, which is a feed stream that contains the target contaminant, with an outlet where the treated stream exits.

Key set-up considerations

When setting up a fixed bed, several factors need to be considered. These factors include bed height, which affects pressure drop, flow distribution, and adsorption capacity. Another factor is bed diameter, which influences flow rate, pressure drop, and wall effects. Particle size also impacts adsorption kinetics, pressure drop, and flow distribution, while flow rate affects residence time, adsorption capacity, and pressure drop.
Out of these parameters, initial adsorbate concentration, bed height and flow rate are most feasible parameters, as most of researchers are recently working on these parameters and utilising them to remove various types of pollutants like dyes, metal, hazardous waste, etc. using natural and synthetic adsorbents (Patel, 2019).

UV-Vis spectrophotometer

To estimate concentration of malachite green in solutions, UV (ultraviolet and visible) vis spectrophotometer (UV-1800) was used. The dye stock solution was prepared by dissolving 0.5g of MG in 1000 mL of water in conical flasks, having effective concentration as 0.5g/L. Working dilutions were prepared using dilution formula. The absorbance of solutions before and after adsorbent applications was measured at 460 nm, with the blank solution measured as 0.175.

Characterisation of adsorbents

Characterization of adsorbents is essential for understanding their structure and suitability for adsorption processes. This includes Brunauer-Emmett-Teller BET analysis, Scanning Electron Microscopy (SEM), and Fourier-Transform Infrared Spectroscopy (FTIR).

Brunauer-Emmett-Teller BET analysis

This analysis measures the specific surface area of the adsorbent. This technique involves the adsorption of nitrogen gas onto the adsorbent's surface under controlled conditions, providing insights into the surface area, pore size distribution, and total pore volume. These parameters are crucial for assessing the adsorption capacity and overall behaviour of the adsorbent material.

Bet surface area analysis

BET analysis is a precise method for evaluating the specific surface area of materials through nitrogen multilayer adsorption, measured as a function of relative pressure using a fully automated analyser. It can be performed using either single-point BET, which determines the specific surface area from a single point on the isotherm, or multipoint BET, which requires at least three data points for a more detailed analysis.

By assessing both external surface area and pore area, this technique calculates the total specific surface area in m^2/g, providing crucial insights into the effects of surface porosity and particle size in various applications (Pradeep et al., 2016).

Barrett-Joyner-Halenda (BJH) method

The Barrett-Joyner-Halenda (BJH) method, introduced in 1951, was initially designed for adsorbents with wide pores and broad pore size distributions, but it has since been proven effective for analysing virtually all types of porous materials. The BJH model assumes that pores have a cylindrical shape, with the pore radius equal to the sum of the Kelvin radius and the thickness of the adsorbed film on the pore wall.

This technique can be used to determine pore area and specific pore volume through adsorption and desorption methods, and it characterises pore size distribution independently of the external surface area, which is influenced by the sample's particle size (Pradeep et al., 2016).

Scanning electron microscopy (SEM)

This method offers a detailed look at the adsorbent's surface morphology and structure by scanning it with a focused electron beam. The resulting high-resolution images reveal details about the surface texture, particle size, and the presence of pores or other irregularities. Understanding these physical characteristics is vital for interpreting how the adsorbent interacts with the adsorbate.

Fourier-transform infrared spectroscopy (FTIR)

This method is used to identify the functional groups present on the adsorbent's surface. It works by measuring how the sample absorbs infrared radiation, which causes vibrations in specific molecular bonds. Each type of functional group absorbs certain wavelengths, creating characteristic peaks in the spectrum. This information is valuable for understanding the nature of interactions between the adsorbent and the adsorbate, such as how malachite green binds to the surface of activated carbon.

Breakthrough curve analysis

The breakthrough analysis consists of the breakthrough point, which is the time when contaminant concentration exceeds a set threshold. When dealing with a significant quantity of samples, it is advantageous to utilise a breakthrough curve to analyse the adsorption, kinetics, and separation factor of porous materials in a fixed bed (So and Oh, 2024).

The breakthrough point occurs when the adsorbate begins to exit from the end of the column, at a concentration that is usually equal to 5 or 10% of its initial concentration (Patel, 2019). The breakthrough curve is generally expressed by Ct/C0 as a function of time or volume of the effluent. The effluent volume can be calculated from the equation as follows; Veff= Qttotal, where Q is the volumetric flow rate and ttotal is the total flow time (min).

Mass transfer zone and column efficiency

In fixed-bed adsorption, the concentrations of the adsorbate in both the fluid and solid phases change over time and along the bed's length. Initially, mass transfer primarily occurs near the inlet of the bed, where the fluid first encounters fresh adsorbent. If the adsorbent is free of adsorbate at the beginning, the fluid-phase concentration decreases exponentially with distance, approaching zero before reaching the end of the bed.

The region within the bed where significant adsorption occurs, characterized by a notable change in concentration, is known as the mass transfer zone (MTZ) or length of the mass transfer zone (LMTZ). The majority of adsorption at any given time takes place within this relatively narrow zone. The boundaries of the MTZ are often defined where the outlet-to-inlet concentration ratio, Cexit/Cin ranges between 0.95 and 0.05 (Al Mesfer et al., 2020).

Column adsorption models

Several mathematical models have been developed to assess the efficiency and applicability of column models (Patel, 2019). The models employed for this study were Thomas, Adams-Bohart, and Yoon Nelson models. Different parameters were derived from each model which described the performance of the adsorption column (Omitola et al., 2022).

MATERIALS AND METHOD

Materials

For this experimental setup, the various essential equipment and materials listed in table 1 below were utilized.

Table 1 shows materials used for the experimental work and their uses.

S/N	Materials	Usage
1	Analytical balance	To accurately weigh a sample of malachite green pigment
2	pH meter	To determine the pH values of the samples, which ensures optimal conditions for the adsorption process.
3	Beakers and measuring cylinders	For holding solutions and providing precise measurements of solutions.
4	Retort stand	To support the experimental setup, ensuring stable and organized experimentation
5	High quality water	To prepare the solutions
6	Fixed bed column	To conduct the main reactions in the adsorption experiments
7	Sawdust	Used as precursor for the activated carbon
8	Sawdust-derived activated carbon	Used as an adsorbent.
9	Malachite green pigment	Used as target compound
10	Pipes	To extract the treated effluent from the stationary bed column.

TIJERT
E-ISSN 3027-1770
P-ISSN 3026-8095

11	Stopwatch	To accurately measure time during various stages of the experiments.
12	Test tubes	To gather samples of the effluent for analysis.
13	Magnetic stirrer	To ensure uniform mixing of the solutions.
14	Funnel	To transfer solutions from the beaker to the separating funnel.
15	Conical flask	To collect solutions from the outlet stream of the fixed bed column.
16	Valve-equipped separating funnel	To effectively direct liquids into the column.
17	Muffle furnace	To heat sawdust to extremely high temperatures. It was essential for activating the sawdust.
18	Autoclave	To decontaminate and sterilize the sawdust, ensuring that the experimental conditions are uncontaminated.
19	H2SO4	To activate the sawdust, which enhances its adsorptive properties.
20	Oven	To dry the sawdust-derived activated carbon samples.

Preparation of sawdust activated carbon

Sawdust was gathered from a furniture workshop at Eku, Delta State, and dried in an oven at 105°C for 3 hours to reduce residual moisture content. The dried sawdust was crushed and charged into a muffle furnace to carbonize at 400°C for 60 minutes. After carbonization, it was crushed further and sieved through a 500 µm sieve. Chemical activation was carried out using 0.5M H_2SO_4. About 250 g of the sample was added to 500 ml of 0.5 M H_2SO_4 solution, boiled for 60 minutes, and allowed to soak in the solution for 24 hours. The sample was then filtered and washed with clean water until a pH of 7 was achieved. Finally, the sample was dried in an oven and stored until use.

Preparation of malachite green pigment solution

A solution of 0.5 g/L was prepared by adding 0.5 g of malachite green pigment into a conical flask containing 1000 ml of water and was stirred until the dye particles were completely dissolved. The solution was filtered and then stored in a clean container. Other working solutions were prepared in the same way.

Experimental setup of the fixed bed column

One of the pieces of equipment used in a continuous adsorption process is a fixed bed column. In this setup, the column was uniformly packed with sawdust-derived

activated carbon, which was supported by glass wool. The column was equipped with inlet and outlet valves. Malachite green pigment solution was added into the fixed bed column from a beaker through a separating funnel. The solution entered the column from the top and flowed downward through it.

Measurements of dye concentrations from the outlet stream

The concentration of malachite green dye in the outlet stream was measured using a UV-Vis spectrophotometer. This technique allows for precise monitoring of dye concentration in the solution, based on the absorption characteristics of malachite green at a specific wavelength.

Fixed-bed adsorption experiments were carried out at bed heights of 5.00, 2.50, and 1.25 cm, each in triplicate (n = 3 independent runs) to ensure reproducibility, with outlet samples collected every 30 minutes and analyzed in technical triplicate using a UV–Vis spectrophotometer at 460 nm.

Instrument and reagent blanks, calibration curves (≥5 standards, duplicate runs, R^2 reported), and periodic drift checks were used as error controls, alongside blank column runs to confirm absence of system adsorption. Flow rate (5 ml/min) was monitored for each run, and any deviations exceeding 5% from set conditions led to repetition of the run.

Data processing, plotting, and model fitting were performed in Microsoft Excel for the web (Microsoft 365, continuously updated version) with Data Analysis ToolPak and Solver, reporting fitted parameters with goodness-of-fit (R^2).

The experiment examined the impact of different bed heights and the quantity of adsorbent. The amount of adsorbent used is an important factor in figuring out how well it can hold a certain amount of adsorbate (Malakootian & Heidari, 2018). The study looked at how different amounts of adsorbent affected the adsorption of malachite green onto activated carbon by using three bed heights (5 cm, 2.5 cm, and 1.25 cm) for the same 30-minute period. The amount of MG adsorbed by the adsorbent increased with bed height, suggesting that greater bed depths provide more active sites for adsorption. These findings demonstrate that bed height significantly affects the adsorption process.

RESULTS AND DISCUSSION

Fourier transform infrared spectroscopy

Figure 4 displays the FTIR spectra for the activated carbon. The peak at 1677.58 cm^{-1} provides details on the availability of the carbon-carbon double bond (C=C), which is characteristic of alkenes. The peak at 722.16 cm^{-1} indicates the presence of a strong carbon-carbon double bond. The peak at 518.88 cm^{-1} provides details

on the availability of C-1 aliphatic iodo compounds. The peak at 463.21 cm^{-1} shows the functional group of S-S stretch aryl disulfides. The analyses above give knowledge about the functional groups that are responsible for the attachment of adsorbates to its surface area and can be inferred from the existence of distinctive frequencies (Nullah and Muhhamad, 2021). The peaks of adsorption indicated that there are some functional groups on the surface of an adsorbent that can react with the various adsorbates in the solution (Bedada *et al.*, 2020).

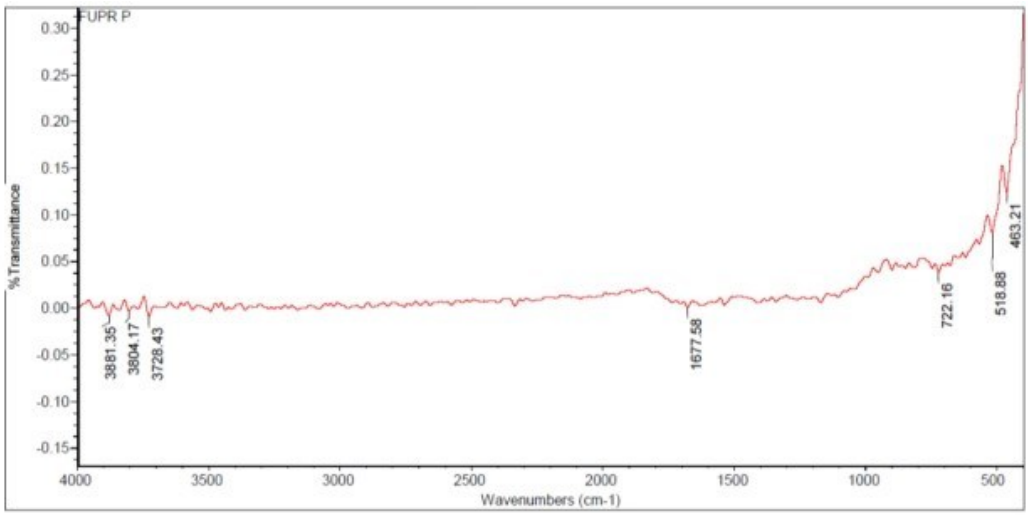

Figure 1: FTIR Spectra for sawdust activated carbon.

Table 2: Analysis of FTIR Spectra for sawdust activated carbon.

Wave number (cm^{-1})	Intensity	Functional Group	Assignment	Information
463.21	0.124	S – S	Aryl disulfides	Stretch
518.88	0.0814	C – I	Aliphatic iodo compounds	Stretch
722.16	0.0385	C = C	Bending alkene	Strong
1677.58	0.00089	C = C	Alkene	Weak, stretching,

BET characterization

The BET analysis showed that the surface area of the sawdust activated carbon was 333.510 m^2/g, measured using nitrogen adsorption-desorption isotherm at 77.350 K. Compared to many locally prepared activated carbons, the adsorbent is slightly superior in terms of the surface area. For instance, the surface area of bentonite is 265 m^2/g (Tebeje *et al.*, 2022), Parthenium hysterophorus-derived activated carbon is 268 m^2/g (Bedada *et al.*, 2020), and Fe_3O_4-GO is 296 m^2/g (Moges

et al., 2022). The higher surface area of the developed adsorbent highlights its enhanced porosity and potential for improved performance in adsorption-related applications. This improvement can be attributed to optimized synthesis conditions and material selection. The findings underline its competitive edge over existing alternatives in the market.

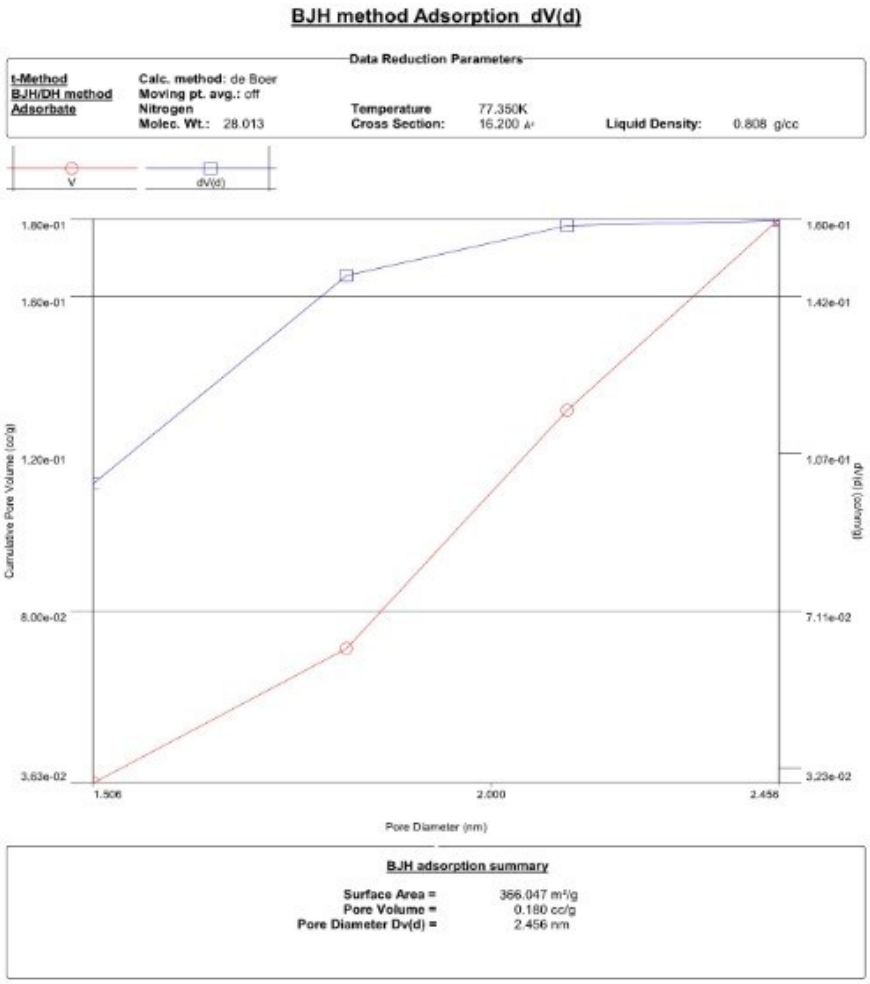

Figure 2: BJH method Adsorption.

Figure 3: Multi point BET plot for sawdust-derived activated carbon.

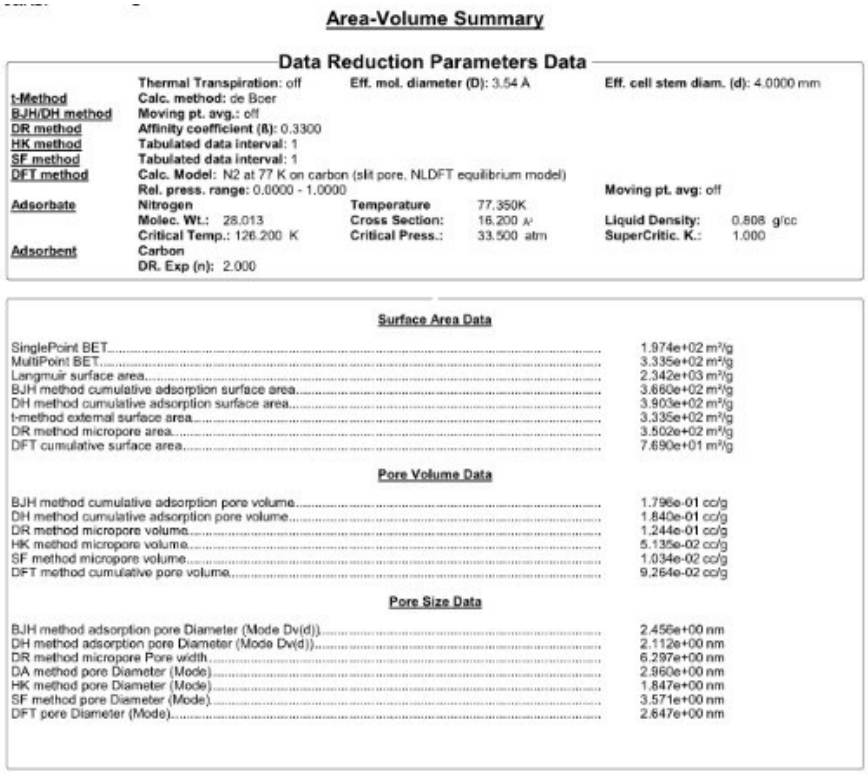

Area-Volume Summary

Data Reduction Parameters Data

	Thermal Transpiration: off	**Eff. mol. diameter (D):** 3.54 Å	**Eff. cell stem diam. (d):** 4.0000 mm
t-Method	**Calc. method:** de Boer		
B-JH/DH method	**Moving pt. avg.:** off		
DR method	**Affinity coefficient (ß):** 0.3300		
HK method	**Tabulated data interval:** 1		
SF method	**Tabulated data interval:** 1		
DFT method	**Calc. Model:** N2 at 77 K on carbon (slit pore, NLDFT equilibrium model)		
	Rel. press. range: 0.0000 - 1.0000		**Moving pt. avg:** off
Adsorbate	**Nitrogen**	**Temperature** 77.350K	
	Molec. Wt.: 28.013	**Cross Section:** 16.200 Å²	**Liquid Density:** 0.808 g/cc
	Critical Temp.: 126.200 K	**Critical Press.:** 33.500 atm	**SuperCritic. K.:** 1.000
Adsorbent	**Carbon**		
	DR. Exp (n): 2.000		

Surface Area Data

SinglePoint BET	1.974e+02 m²/g
MultiPoint BET	3.335e+02 m²/g
Langmuir surface area	2.342e+03 m²/g
BJH method cumulative adsorption surface area	3.660e+02 m²/g
DH method cumulative adsorption surface area	3.903e+02 m²/g
t-method external surface area	3.335e+02 m²/g
DR method micropore area	3.502e+02 m²/g
DFT cumulative surface area	7.690e+01 m²/g

Pore Volume Data

BJH method cumulative adsorption pore volume	1.796e-01 cc/g
DH method cumulative adsorption pore volume	1.840e-01 cc/g
DR method micropore volume	1.244e-01 cc/g
HK method micropore volume	5.135e-02 cc/g
SF method micropore volume	1.034e-02 cc/g
DFT method cumulative pore volume	9.264e-02 cc/g

Pore Size Data

BJH method adsorption pore Diameter (Mode Dv(d))	2.456e+00 nm
DH method adsorption pore Diameter (Mode Dv(d))	2.112e+00 nm
DR method micropore Pore width	6.297e+00 nm
DA method pore Diameter (Mode)	2.960e+00 nm
HK method pore Diameter (Mode)	1.847e+00 nm
SF method pore Diameter (Mode)	3.571e+00 nm
DFT pore Diameter (Mode)	2.647e+00 nm

Figure 4. Summary of BET analysis

SEM EDS analysis

SEM was used to examine the microscopic structure and the surface morphology of activated carbon fiber (Kunusa *et al.*, 2021). The surface of activated carbon was zoomed in on at various levels, showing a pore size of 537 µm at 15.00 KV, and different sizes of pores were found on the surface of the adsorbent. SEM results showed a highly porous structure with a hollow shape, indicative of activated carbon. The pores were visible but appeared relatively small, suggesting incomplete development or blockage by residual impurities. Several small, shiny particles were seen, which matched the trace elements found in the EDS analysis, like aluminum (Al), silicon (Si), and sodium (Na). These impurities likely contribute to partial pore occlusion.

The formation of pores and the observed variation in pore size and shape are attributed to the depolymerization of lignocellulosic components and the release of volatile organic substances during the carbonization and activation process. This process creates a carbon structure with tiny holes, but how many and how

big these holes are depending on how well impurities are removed and the conditions used during activation.

The spectrum visually aligned with the tabular data, showing a strong peak for carbon and smaller peaks for other trace elements. The high carbon content confirmed the successful conversion of sawdust into activated carbon.

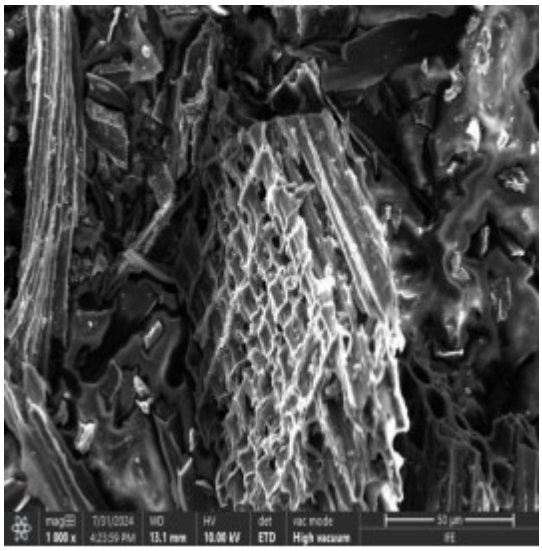

Element Number	Element Symbol	Element Name	Atomic Conc.	Weight Conc.
6	C	Carbon	96.49	94.84
7	N	Nitrogen	2.54	2.91
13	Al	Aluminum	0.22	0.49
14	Si	Silicon	0.18	0.41
11	Na	Sodium	0.17	0.32
12	Mg	Magnesium	0.12	0.24
19	K	Potassium	0.06	0.19
16	S	Sulfur	0.07	0.18
17	Cl	Chlorine	0.06	0.17
15	P	Phosphorus	0.06	0.16
20	Ca	Calcium	0.02	0.08
22	Ti	Titanium	0.00	0.00
26	Fe	Iron	0.00	0.00

FOV: 537 µm, Mode: 15kV - Image, Detector: BSD Full.

Figure 5: SEM analysis for sawdust activated carbon

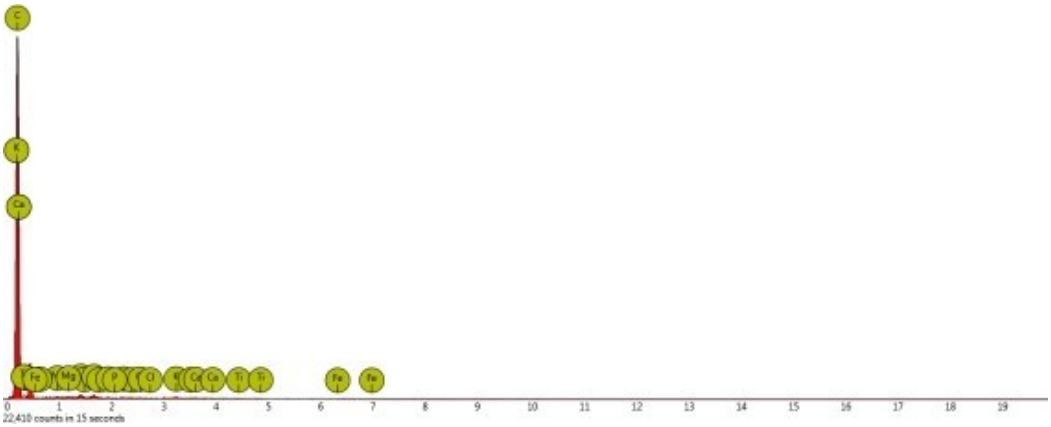

Figure 6: EDS analysis for sawdust activated carbon

Fixed bed adsorption experiment

Absorbance

Table 3 displays the absorbance values of effluent solutions at various bed heights, measured at a wavelength of 460 nm. The table revealed the time interval for the experiments and absorbance at respective bed heights of 1.25 cm, 2.5 cm, and 5 cm.

Table 3: Absorbance at various bed heights.

Time (minutes)	Absorbance 1.25cm	Absorbance 2.50cm	Absorbance 5.00cm
0	0.003	0.004	0.003
30	0.003	0.004	0.003
60	0.003	0.004	0.003
90	0.003	0.004	0.003
120	0.005	0.005	0.003
150	0.007	0.005	0.003
180	0.016	0.006	0.004
210	0.052	0.007	0.004
240	0.086	0.007	0.004
270	0.116	0.014	0.004
300	0.131	0.053	0.006
330	0.165	0.095	0.018
360	0.172	0.132	0.041
390	0.174	0.172	0.083
420	0.174	0.174	0.136
450	0.174	0.174	0.159
480	0.174	0.174	0.172
510	0.174	0.174	0.174
540	0.174	0.174	0.174
570	0.174	0.174	0.174
600	0.174	0.174	0.174

Effluent concentration

The initial concentration of the solution was measured to be 500 mg/L. Table 4 shows the effluent concentrations with respect to time.

Table 4: Effluent concentrations for respective bed heights with respect to time

Time (min)	Ct for 1.25cm	Ct for 2.50cm	Ct for 5.00cm
30	12.67379	15.52272	12.67379
60	12.67379	15.52272	12.67379
90	12.67379	15.52272	12.67379
120	18.37165	18.37165	12.67379
150	24.06951	18.37165	12.67379
180	49.70988	21.22058	15.52272
210	152.27136	24.06951	15.52272
240	249.13498	24.06951	15.52272
270	334.60288	44.01202	15.52272
300	377.33683	155.1203	21.22058
330	474.20045	274.7754	55.40774
360	494.14296	380.1858	120.9331
390	499.84082	494.143	240.5882
420	499.84082	499.8408	391.5815
450	499.84082	499.8408	457.1069
480	499.84082	499.8408	494.1430
510	499.84082	499.8408	499.8408
540	499.84082	499.8408	499.8408
570	499.84082	499.8408	499.8408
600	499.84082	499.8408	499.8408

Breakthrough Curves Concentration

Breakthrough curves

The breakthrough curve represents the plot of the ratio of concentration at time to the initial concentration (Ct/Co) against time. It is used to visualize how a contaminant passes through a medium over time. The adsorption of malachite green using sawdust-based activated carbon was evaluated through breakthrough curves. The wastewater flow was halted when the effluent's Malachite Green concentration (Ct) reached 98% of its initial concentration (Co) (Sizirici and Yildiz, 2020).

E-ISSN 3027-1770
P-ISSN 3026-8095

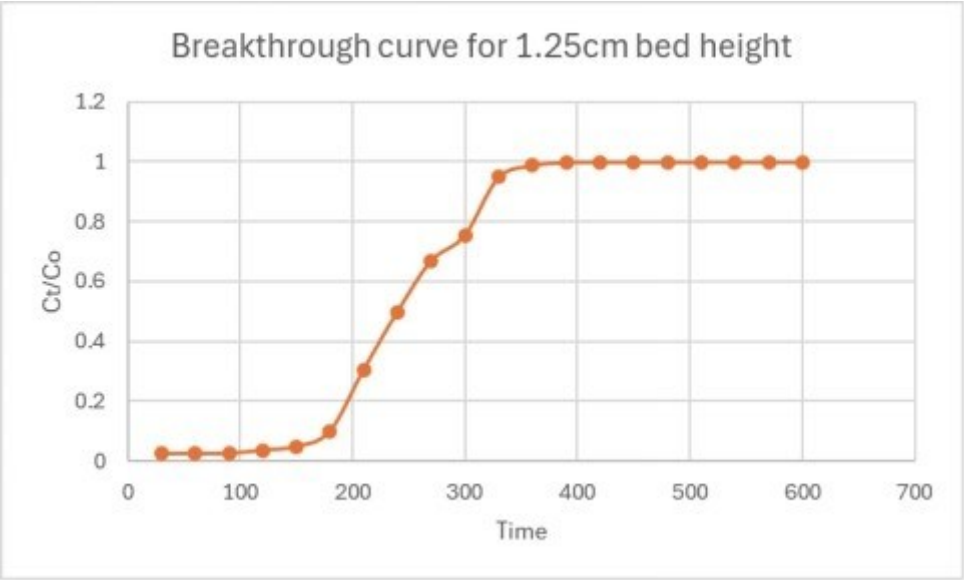

Figure 7: Graph of Ct/Co against Time for 1.25cm bed height.

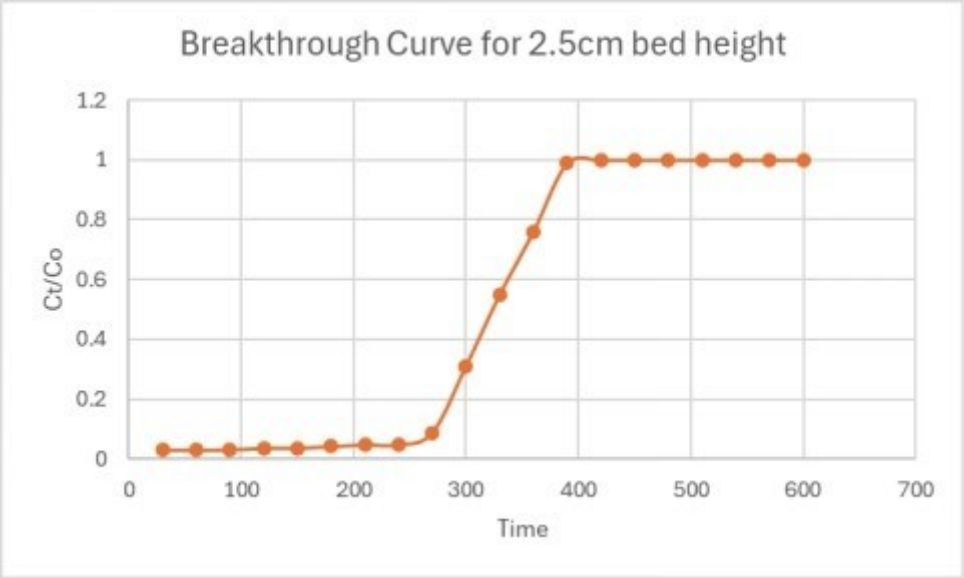

Figure 8: Graph of Ct/Co against Time for 2.5Cm bed height.

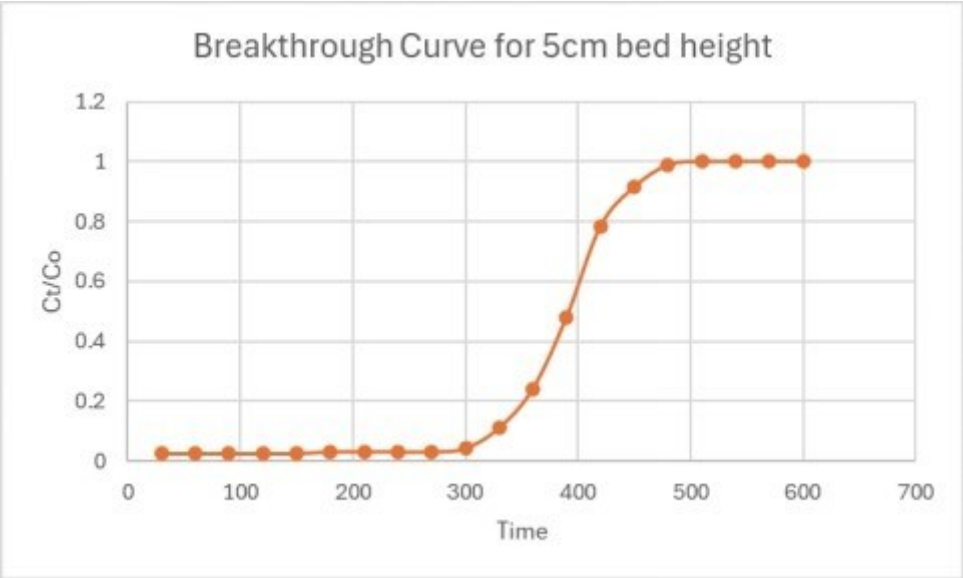

Figure 9: Graph of Ct/Co against Time for 5cm bed height.

Breakthrough curve Analysis

According to Al Mesfer *et al.*, 2020, the Time equivalent to total capacity of the bed (t_t) was estimated using

$$t_t = \int_0^{ttotal} (1 - \frac{C}{Co})dt \quad (1)$$

The time equivalent to usable capacity of the bed, tu was estimated using

$$t_u = \int_0^{tb} (1 - \frac{C}{Co})dt \quad (2)$$

The fraction of the total bed capacity/ length utilized up to breakpoint is estimated using

tu/tt

The length of bed used up to the break point is estimated by:

$H_B = (tu/tt)\, H_T$ (3)

Where H_T is total length of bed, H_B is the length of bed used up to breakpoint.

The length of unused bed, H_{UNB} is the unused fraction times total length. It represents the mass transfer section of the bed. It is estimated using

$H_{UNB} = (1- tu/tt)\, H_T$ (4)

The total amount of malachite green adsorbed, q_{total}(mg), for a feed concentration of 500mg/L, and flow rate of 5ml/min, was determined by calculating the area under the plot of adsorbed concentration (C_o-C_t)(mg/L) against time (min). According to (Sizirici and Yildiz, 2020), the expression is shown as:

q_{total} (mg)= Q.A/1000 = Q/1000 $\int_0^{ttotal}$ $C_{ad}dt$ (5)

Where Q represents the volumetric flow rate (ml/min), $C_{ad} = C_o - C_t$, where C_o is the initial concentration, and C_t, is the concentration (mg/L) at time. The dynamic adsorption capacity, (mg/g), was calculated as:

qe= qtotal/m (6)

Where m denotes the mass of AC packed in the column (g).

The removal efficiency of Malachite Green was assessed by calculating the ratio of the total amount adsorbed in the column to the total amount introduced, as follows:

Efficiency=(qtotal/ (Co Q/100 ttotal))x 100 (7)

Where C_o is the influent concentration (mg/L), Q is the flow rate (ml/min), and t_{total} is the total time until exhaustion (min).

Table 5 shows the times for breakthrough and exhaustion, the time that equals total capacity, the time that equals usable capacity, the fraction of total bed capacity used, the length of the bed that was used, the length of the bed that was not used, the total amount of MG adsorbed (qtotal), the dynamic adsorption capacities, and the removal efficiency of MG for bed heights of 1.25 cm, 2.5 cm, and 5.0 cm.

Table 5 shows the trends in column performance for the fixed bed adsorption column.

Bed heights (cm)	Breakthrough time (t_b) (mins)	Exhaustion time (t_d) (mins)	t_t (mins)	t_u (mins)	T_u/t_t (%)	H_B (cm)	H_{UNB} (cm)	q_{total} (mg)	q_e (mg/g)	Removal Efficiency (%)
1.25	180	390	236.6	168	71	0.9	0.35	531.707	221.54	54.53
2.5	270	420	309.4	254	82	2.05	0.45	713.552	148.34	67
5.0	330	510	375.7	314.6	83.7	4.19	0.81	877.51	91.22	68.82

Table 5 shows the trends in column performance for the fixed bed adsorption column. As the bed heights increased from 1.25 cm to 5.0 cm, both tb and td increased. This implies that taller beds delay the breakthrough time and allow for a longer exhaustion time. This is expected because a taller bed provides a larger volume of adsorbent, allowing it to hold onto the adsorbate longer before saturation. The total and usable capacity of the bed increased with bed height, as the adsorption capacity decreased with increasing bed heights, implying that although a taller bed can adsorb more total malachite green, it does so less

E-ISSN 3027-1770
P-ISSN 3026-8095

efficiently on a per-unit basis. The fraction of total bed capacity rose with bed height, suggesting that higher beds utilize their total capacity more effectively.
The length of the bed used for adsorption increased with bed height, while the unused bed stayed relatively low. This indicated that with a higher bed, the column utilized more of the bed height effectively. The total adsorbed malachite green increased with bed height, suggesting that higher beds are more effective at removing larger quantities of dye in total. Removal efficiency improved slightly with bed height, indicating that a higher bed has a higher percentage removal efficiency. This is expected because the adsorbate has more contact time with the adsorbent in a taller bed, allowing for more effective removal.

Effect of Adsorbent Bed Height on Breakthrough Curves

The effect of bed height on column performance is illustrated by the breakthrough curves in figures 4.7, 4.8, and 4.9. It is revealed that as bed height was increased from 1.25 to 2.5 and 5 cm, the time to reach breakthrough increased from 180 mins to 270 and 330 mins, respectively.
According to Patel, 2019, this variation is a result of an increase in the surface area and the number of binding sites available for adsorption. Increasing the bed height from 1.25 to 5 cm expanded the number of available adsorption sites, leading to improved removal efficiency of the column (Omitola *et al.,* 2022). It was found that as the bed height increased, MG had more time for contact, resulting in an increased higher dye removal yield of MG. The exhaustion time for the adsorbent bed was found to increase from 390 mins to 420 mins and 510 mins as bed height increased from 1.25 to 2.5 and 5 cm, respectively. Since slower exhaustion of the adsorbent bed is more desirable, higher bed height is preferable for this operation (Omitola *et al.,* 2022).

E-ISSN 3027-1770
P-ISSN 3026-8095

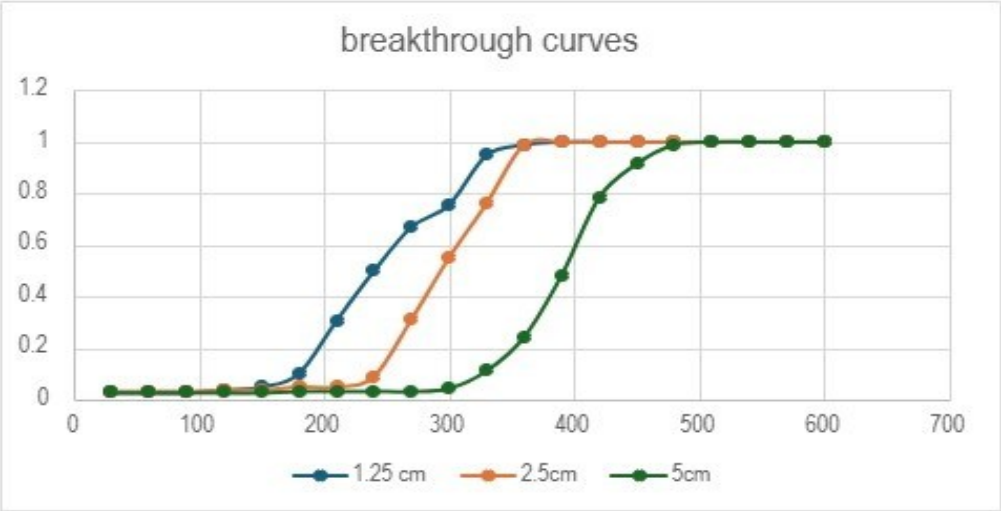

Figure 10 shows a graph of Ct/Co against time for bed heights of 1.25, 2.5, and 5cm.

Column Adsorption Modelling

Thomas model

The Thomas model is one of the most widely used and general models for studying column adsorption processes. It is used to find out the highest amount of adsorbate that can stick to the adsorbent and the rate at which this happens, using information from ongoing column studies (Patel, 2019). The model is based on the assumption that the adsorption process follows Langmuir kinetics, which assumes that adsorption sites are finite and identical and the adsorption process is reversible. The linear model, which has a plot of In (Co/Ct -1) vs t, is shown below

$$\text{In } (Co/Ct - 1) = (K_{TH} q_o X/Q) - K_{TH} C_o t \quad (8)$$

Where Ct and Co are concentrations of MG (mg/L), K_{TH} is the rate constant (L mg-1 min-1), Q is flowrate (L min-1), q_o is total adsorption capacity (mg/g), X is the mass of adsorbent (g).

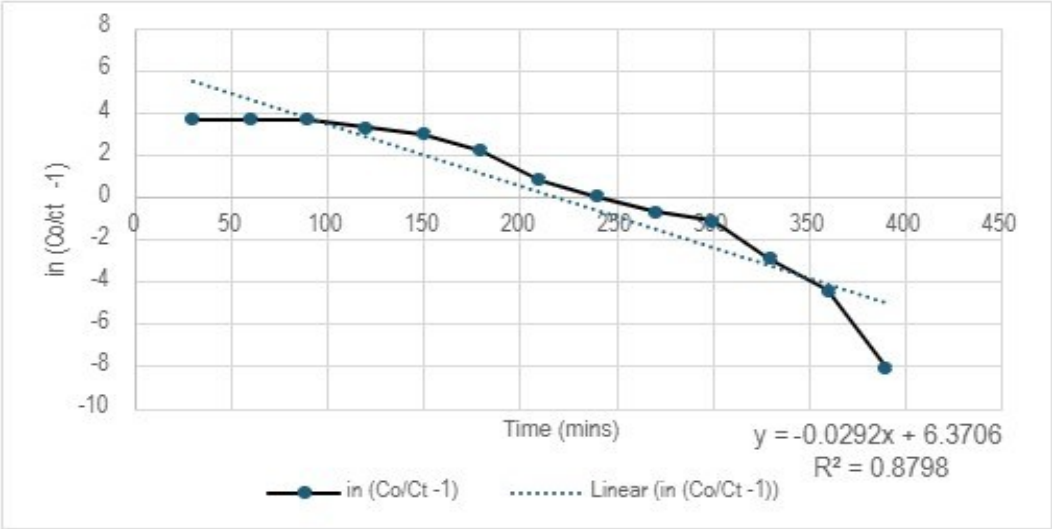

Figure 11: Graph of In (Co/Ct-1) against time for bed height of 1.25cm.

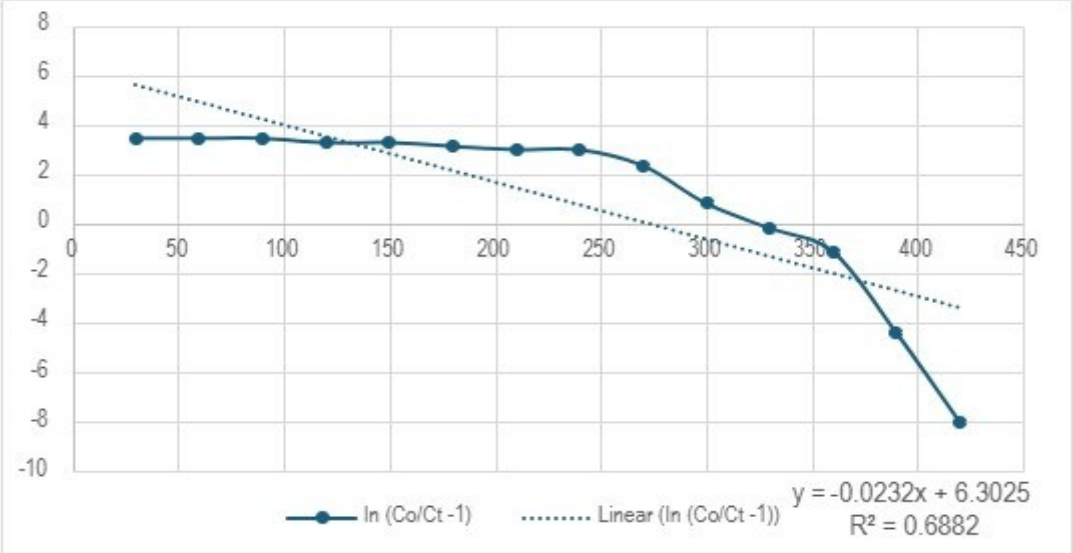

Figure 12: Graph of In (Co/Ct-1) against time for bed height of 2.5cm.

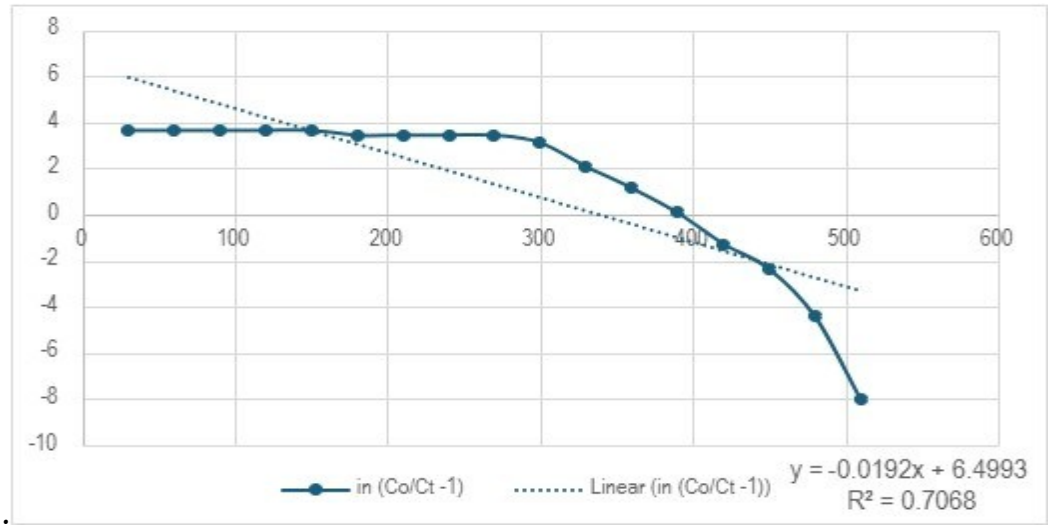

Figure 13: Graph of In (Co/Ct-1) against time for bed height of 5.0cm.

Yoon-Nelson model

The Yoon-Nelson model is a straightforward theoretical model used to describe the adsorption process in column studies. It is applied to predict the time required and the rate constant for a 50% adsorbate breakthrough.

It offers a generalized framework that suggests that the rate of adsorption decreases in direct proportion to the amount of adsorbate already adsorbed and the breakthrough point of the adsorbate on the adsorbent (Patel, 2019). *Mohammad et al. (2014) illustrate the linear model below, displaying a plot of In (Ct/Co-Ct) vs t.*

$$\ln(Ct/Co-Ct) = K_{YN}t - \tau K_{YN} \quad (9)$$

Where K_{YN} (min-1) is the rate constant, and τ(min) is time required for 50% adsorbate breakthrough.

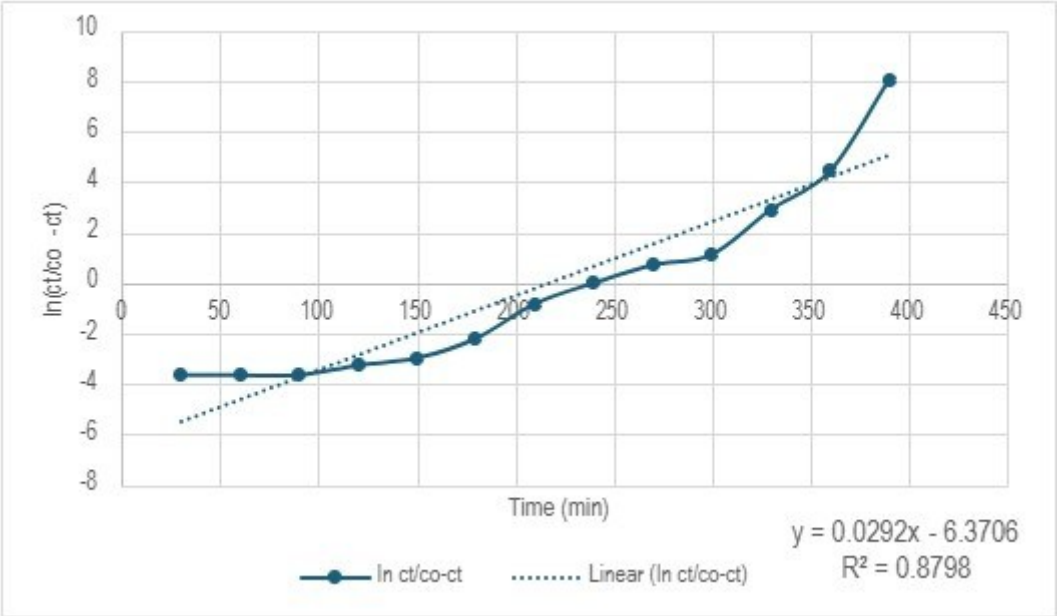

Figure 14: Graph of In (Ct/Co-Ct) against time for bed height of 1.25cm.

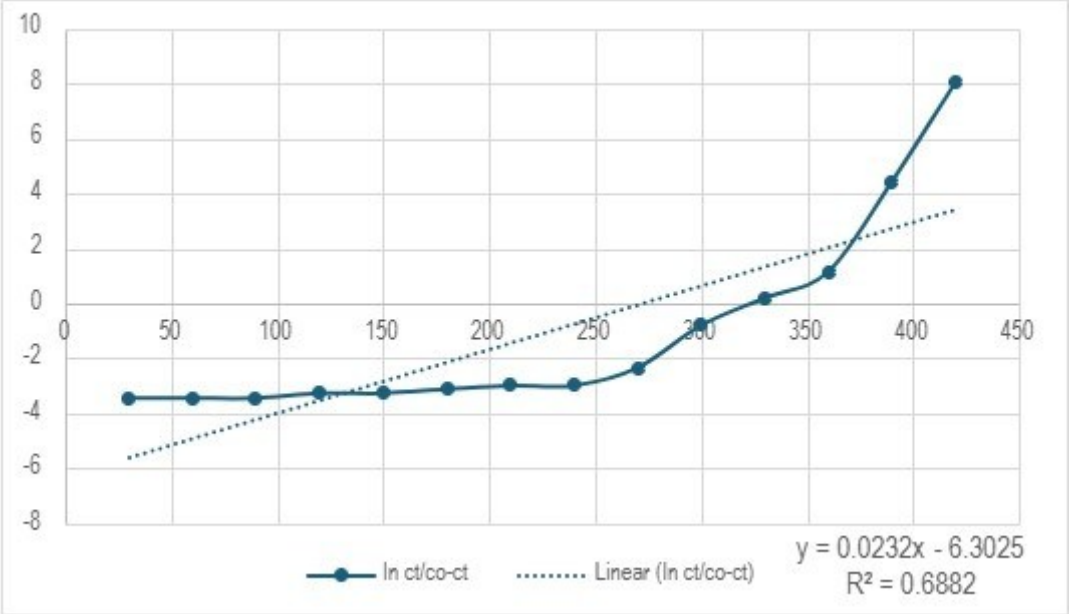

Figure 15: Graph of In (Ct/Co-Ct) against time for bed height of 2.5cm.

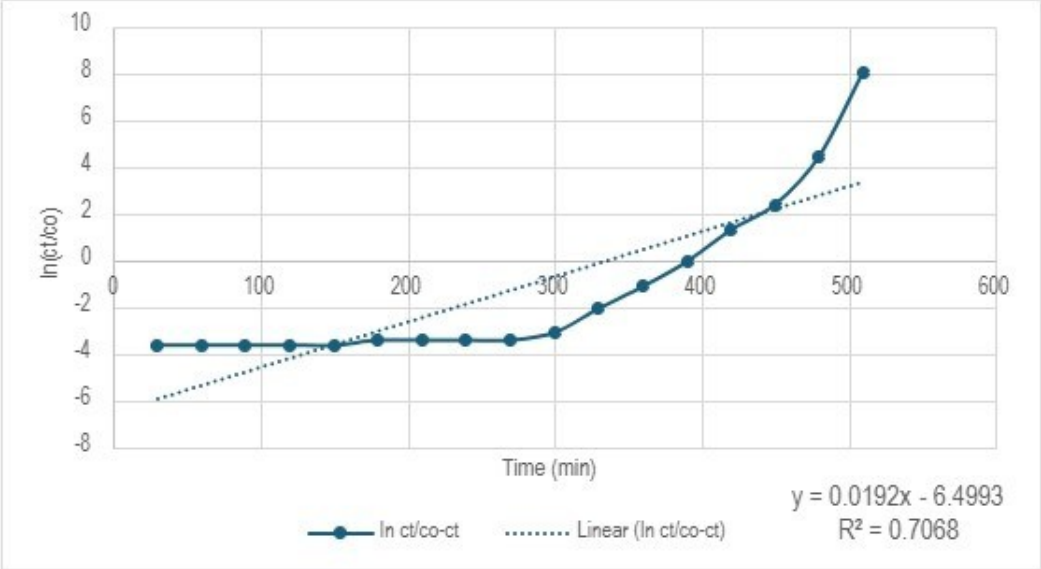

Figure 16: Graph of In (Ct/Co-Ct) against time for bed height of 5.0cm.

Adams-Bohart model

The Adams-Bohart model suggests that two factors influence the rate of adsorption. According to Dorado *et al.,* 2014, the factors involved are the concentration of sorbate and the remaining adsorption capacity of the adsorbent. This model effectively predicts the early stages of adsorption in column systems, providing insights into breakthrough behavior as well as adsorbent exhaustion over time. According to Mohammad *et al.,* 2014, the linear model, which has a plot of In (Ct/Co) vs t, is shown below

$$\ln(Ct/Co) = K_{AB}C_o t - K_{AB}N_o Z/F \quad (10)$$

Where K_{AB} is the rate kinetic constant of the Adams-Bohart model ($Lmg^{-1}\ min^{-1}$), No is the adsorption capacity per unit volume of fixed bed (mg/ml), F is linear velocity (cm/min), and Co and Ct (mg/L) are influent and effluent concentrations, and Z is bed height (cm).

E-ISSN 3027-1770
P-ISSN 3026-8095

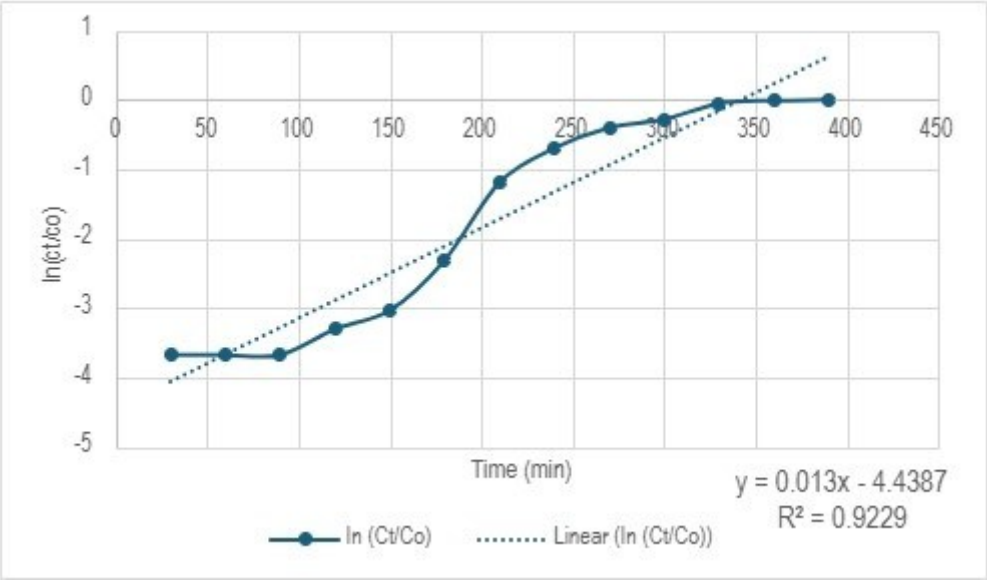

Figure 17: Graph of In (Ct/Co) against time for bed height of 1.25cm.

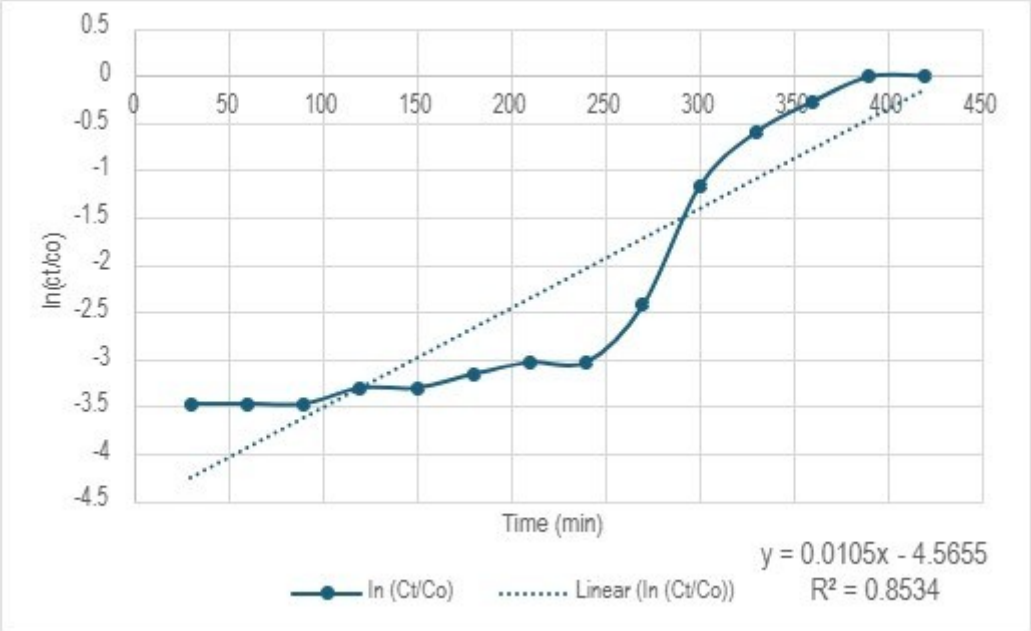

Figure 18: Graph of In (Ct/Co) against time for bed height of 2.5cm.

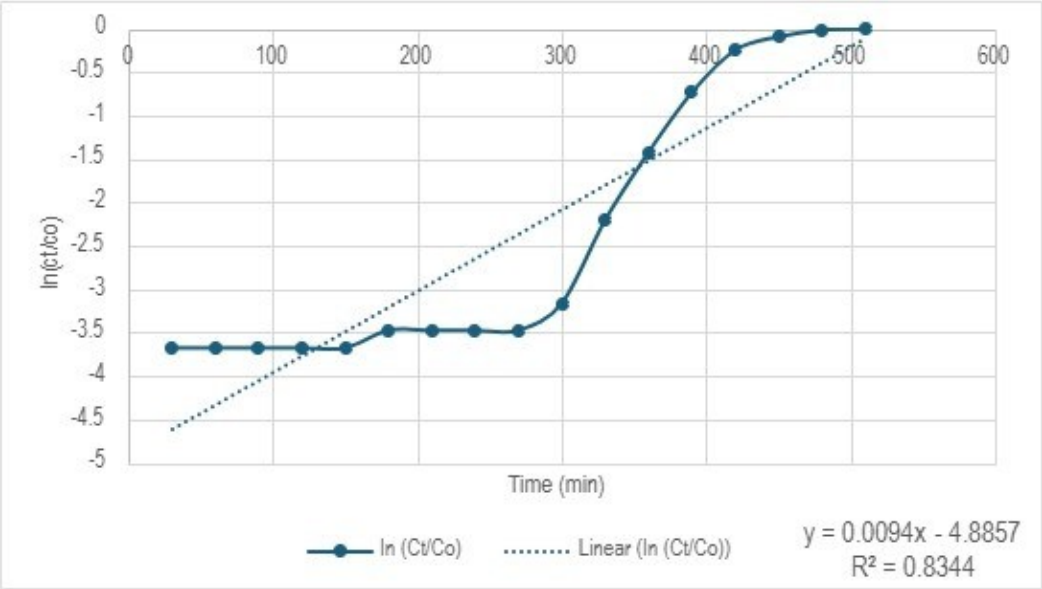

Figure 19: Graph of In (Ct/Co) against time for bed height of 5cm.

Table 6 shows the parameter values for the models at bed heights of 1.25, 2.5, and 5.0cm respectively.

Thomas					Yoon Nelson			Adams-Bohart		
Bed height (cm)	C_o (mg/L)	q_o (mg/g)	K_{th} (L/mg/min)	R^2	K_{YN} (min^{-1})	τ (min)	R^2	K_{AB} (L/mg/min)	N_o (mg/ml)	R^2
1.25	500	227.262	$5.84X10^{-5}$	0.8798	0.0292	218.2	0.8798	$2.6X\ 10^{-5}$	188064.30	0.9229
2.5	500	141.195	$4.64X\ 10^{-5}$	0.6882	0.0232	271.7	0.6882	$2.1X\ 10^{-5}$	119746.54	0.8534
5.0	500	87.969	$3.84X10^{-5}$	0.7068	0.0192	338.5	0.7068	$1.88X\ 10^{-5}$	71570.31	0.8344

Table 6 presents the results for different bed heights (1.25 cm, 2.5 cm, and 5 cm), showing how the Thomas, Yoon-Nelson, and Adams-Bohart models help us understand adsorption capacity, rate constants, and how well the data fits. At 1.25 cm, the Thomas model showed a high adsorption capacity of 227.262 mg/g with an R^2 of 0.8798, while the Yoon-Nelson model had a similar R^2 of 0.8798, with a τ of 218.2 minutes, indicating faster breakthrough. The Adams-Bohart model achieved the highest R^2 of 0.9229, suggesting the best fit for this bed height, with K_{AB} of 2.6x10-5 and N_o of 188064.3.

At 2.5 cm, the Thomas model's adsorption capacity decreased with an R^2 of 0.6882, and the Yoon-Nelson model similarly weakened with an R^2 of 0.6882, while τ increased to 271.7 minutes, indicating slower breakthrough. The Adams-Bohart model, with an R^2 of 0.8534, continued to perform better, adapting more effectively to the increased bed height.

At 5 cm, the Thomas model showed the lowest adsorption capacity of 87.969 and an R^2 of 0.7068, paralleled by the Yoon-Nelson model's reduced fit and extended τ of 338.5 minutes. This indicated that at 5cm, the column had a better performance as similarly reported by Yagub *et al.,* 2014. The decreasing values of adsorption capacity, with K_{YN} values with respect to increasing bed heights, was also reported by Omitola *et al.,* 2022.

With an R-value of 0.8344, the Adams-Bohart model maintained its relative robustness, demonstrating its superior adaptability across various bed heights. The Adams-Bohart model emerges as the most suitable model for describing the experimental data, showing consistently high R^2 values and reliable performance across all bed heights, particularly with the highest R^2 of 0.9229 at 1.25 cm.

CONCLUSION

FTIR, SEM-EDS, and BET analyses confirmed the surface chemistry, morphology, surface structure, surface area, and porosity of the activated carbon. SEM-EDS showed the specific elements found in the area being studied (537 µm) using a 15 kV voltage. The primary element detected is carbon, with 94.84% of the sample by weight, with little traces of phosphorus and calcium.

FTIR provided information about the functional groups present in the sample, with the peak at 1677.58 cm^{-1} providing details on the availability of the carbon-carbon double bond (C=C), which is characteristic of alkenes. The total adsorbed malachite green increased with bed height, suggesting that higher beds are more effective at removing larger quantities of dye in total. Removal efficiency improved slightly with bed height, indicating that a higher bed has higher percentage removal efficiency, with the adsorption capacity decreasing with increased bed heights.

The Thomas, Yoon–Nelson, and Adams–Bohart models were applied, with the Adams–Bohart model emerging as the most suitable for describing the experimental data, consistently yielding the highest R^2 values.

The study establishes that activated carbon derived from sawdust, when employed in a fixed-bed column configuration, offers a highly efficient, economically viable, and environmentally sustainable approach for the removal of malachite green dye from aqueous systems.

The demonstrated adsorption performance showcases its strong potential for integration into large-scale industrial wastewater treatment frameworks, particularly in dye-intensive sectors such as textiles. Beyond the clear cost advantages and its contributions to circular economy strategies through waste-to-resource conversion, the technology's adaptability and operational efficiency

position it as a compelling alternative to more energy- and resource-intensive treatment methods.

Future research should prioritise pilot- and full-scale implementation, investigate regeneration and reuse cycles to enhance longevity and cost-effectiveness, and validate performance using complex industrial effluents. These findings directly advance the study's aim by providing a robust, scalable, and sustainable pathway for pollutant removal, aligning with global imperatives for greener water treatment technologies.

RECOMMENDATIONS

The study has provided valuable insights into the effect of varying bed heights on the flow dynamics and concentration profiles in the experimental setup. However, there are several avenues for further investigation to enhance the reliability and comprehensiveness of the findings:

1. The uniformity of bed packing could be further investigated, as variations in bed height distribution could lead to irregular flow patterns. Ensuring consistent packing using calibrated tools and protocols will help maintain uniform bed heights across trials.
2. To improve the accuracy of flow rate measurements, it is recommended to implement automated flow control systems.
3. The accuracy of concentration measurements should be addressed by incorporating automated sampling systems and standardising sampling times and procedures. Utilising multiple replicates will further reduce the impact of human errors in data collection.
4. Using high-precision instruments and verifying measurements before each trial can improve consistency in preparing the initial concentration. Additionally, careful mixing should be performed to avoid concentration gradients that could affect the results.
5. To minimise errors in data analysis, implementing a double-check system will reduce transcription and calculation mistakes. Including error analysis in the results will also help quantify uncertainties and improve the reliability of the conclusions.
6. An environmental impact assessment should be conducted to evaluate the influence of external factors, such as temperature and humidity, on the experiment. Maintaining a controlled environment will help mitigate any variables that could affect the flow behaviour and concentration profiles.

REFERENCES

Abewaa, M., Mengistu, A., Takele, T., Fito, J., & Nkambule, T. (2023). Adsorptive removal of malachite green dye from aqueous solution using Rumex abyssinicus derived activated carbon. *Scientific Reports*, *13*(1). https://doi.org/10.1038/s41598-023-41957-x

Al-Ghouti, M. A., & Da'ana, D. A. (2020). Guidelines for the use and interpretation of adsorption isotherm models: A review. Journal of Hazardous Materials, 393, 122383. https://doi.org/10.1016/j.jhazmat.2020.122383

Al Mesfer, M. K., Danish, M., Khan, M. I., Ali, I. H., Hasan, M., & Jery, A. El. (2020). Continuous fixed bed co2 adsorption: Breakthrough, column efficiency, mass transfer zone. *Processes*, *8*(10), 1–16. https://doi.org/10.3390/pr8101233

Al-Tohamy, R., Ali, S. S., Li, F., Okasha, K. M., Mahmoud, Y. A. G., Elsamahy, T., Jiao, H., Fu, Y., & Sun, J. (2022). A critical review on the treatment of dye-containing wastewater: Ecotoxicological and health concerns of textile dyes and possible remediation approaches for environmental safety. In *Ecotoxicology and Environmental Safety* (Vol. 231). Academic Press. https://doi.org/10.1016/j.ecoenv.2021.113160

Bedada, D., Angassa, K., Tiruneh, A., Kloos, H., & Fito, J. (2020). Chromium removal from tannery wastewater through activated carbon produced from Parthenium hysterophorus weed. *Energy, Ecology and Environment*, *5*(3), 184–195. https://doi.org/10.1007/s40974-020-00160-8

Boucherdoud, A., Kherroub, D. E., Benderdouche, N., Boucherdoud, A., Kherroub, D. E., Bestani, B., Benderdouche, N., Douinat, O., & History, A. (n.d.). Fixed-bed adsorption dynamics of methylene blue from aqueous solution using alginate-activated carbon composites adsorbents ARTICLE INFO ABSTRACT/RESUME. *Algerian Journal of Environmental Science and Technology Month Edition*. www.aljest.org

Chopra, N. K., & Sondhi, S. (2022). Biodegradation of malachite degradation by laccsae from Bacillus licheniformis NS2324. *International Journal of Health Sciences*, 8517–8527. https://doi.org/10.53730/ijhs.v6ns2.7195

Crini, G., & Lichtfouse, E. (2019). Advantages and disadvantages of techniques used for wastewater treatment. Environmental Chemistry Letters, 17, 145–155. https://doi.org/10.1007/s10311-018-0785-9

Dawood, S., Sen, T. K., & Phan, C. (2018). Performance and dynamic modelling of biochar and kaolin packed bed adsorption column for aqueous phase methylene blue (MB) dye removal. Environmental Technology, 40(28), 3762–3772. https://doi.org/10.1080/09593330.2018.1491065

Dim, P. E., Mustapha, L. S., Termtanun, M., & Okafor, J. O. (2021). Adsorption of chromium (VI) and iron (III) ions onto acid-modified kaolinite: Isotherm, kinetics and thermodynamics studies. *Arabian Journal of Chemistry*, *14*(4). https://doi.org/10.1016/j.arabjc.2021.103064

Duduna, W.-E., Akeme, N., & Zinipere, T. M. (2019). Comparison Of Various Adsorption Isotherm Models For Allium Cepa As Corrosion Inhibitor On Austenitic Stainless Steel In Sea Water. *INTERNATIONAL JOURNAL OF SCIENTIFIC & TECHNOLOGY RESEARCH*, *8*, 8. www.ijstr.org

Fito, J., Abewaa, M., Mengistu, A., Angassa, K., Ambaye, A. D., Moyo, W., & Nkambule, T. (2023). Adsorption of methylene blue from textile industrial wastewater using activated carbon developed from Rumex abyssinicus plant. *Scientific Reports*, *13*(1). https://doi.org/10.1038/s41598-023-32341-w

Hummadi, K. K., Luo, S., & He, S. (2022). Adsorption of methylene blue dye from the aqueous solution via bio-adsorption in the inverse fluidized-bed adsorption column using the torrefied rice husk. *Chemosphere*, *287*. https://doi.org/10.1016/j.chemosphere.2021.131907

Ibrahim, H. G., & Al-Meshragi, M. A. (2020). Experimental study of adsorption on activated carbon for CO2 capture. IntechOpen. https://doi.org/10.5772/intechopen.85834

Jabar, J. M., Adebayo, M. A., Odusote, Y. A., Yılmaz, M., & Rangabhashiyam, S. (2023). Valorization of microwave-assisted H3PO4-activated plantain (Musa paradisiacal L) leaf biochar for malachite green sequestration: Models and mechanism of adsorption. Results in Engineering, 18, 101129. https://doi.org/10.1016/j.rineng.2023.101129

Jadhav, A. C., & Jadhav, N. C. (2021). Treatment of textile wastewater using adsorption and adsorbents. In *Sustainable Technologies for Textile Wastewater Treatments* (pp. 235–273). Elsevier. https://doi.org/10.1016/B978-0-323-85829-8.00008-0

Kunusa, W. R., Iyabu, H., & Abdullah, R. (2021). FTIR, SEM and XRD analysis of activated carbon from sago wastes using acid modification. *Journal of Physics: Conference Series*, *1968*(1). https://doi.org/10.1088/1742-6596/1968/1/012014

Lakshmipathy, R., & Sarada, N. C. (2015). Methylene blue adsorption onto native watermelon rind: Batch and fixed bed column studies. Desalination and Water Treatment, 57, 1–14. https://doi.org/10.1080/19443994.2015.1040462

Li, W., Mu, B., & Yang, Y. (2019). Feasibility of industrial-scale treatment of dye wastewater via bio-adsorption technology. Bioresource Technology, 277, 157–170. https://doi.org/10.1016/j.biortech.2019.01.002

Majji, K. R., Kachireddy, V. N. S. R., Kuruva Nandyal, S. K., & Battula, S. R. (2021). Role of nanomaterials: Enhancing the adsorption efficiency of activated carbon in wastewater treatment. In Clean Coal Technologies: Beneficiation, Utilization, Transport Phenomena and Prospective (pp. 215–232). https://doi.org/10.1007/978-3-030-68502-7_9

Malakootian, M., & Heidari, M. R. (2018). Reactive orange 16 dye adsorption from aqueous solutions by psyllium seed powder as a low-cost biosorbent: kinetic and equilibrium studies. *Applied Water Science*, *8*(7). https://doi.org/10.1007/s13201-018-0851-2

Mengistu, A., Abewaa, M., Adino, E., Gizachew, E., & Abdu, J. (2023). The application of Rumex abyssinicus based activated carbon for Brilliant Blue Reactive dye adsorption from aqueous solution. *BMC Chemistry*, *17*(1). https://doi.org/10.1186/s13065-023-01004-2

Moges, A., Nkambule, T. T. I., & Fito, J. (2022). The application of GO-Fe3O4 nanocomposite for chromium adsorption from tannery industry wastewater. Journal of Environmental Management, 305, 114369. https://doi.org/10.1016/j.jenvman.2021.114369

Oladoye, P. O., Ajiboye, T. O., Wanyonyi, W. C., Omotola, E. O., & Oladipo, M. E. (2023). Insights into remediation technology for malachite green wastewater treatment. Water Science and Engineering, 16(3), 261–270. https://doi.org/10.1016/j.wse.2023.03.002

Oladimeji,T.E., Odunoye,B.O., Elehinafe,F.B., Obanla,O.R.,& Odunlami,O.A. (2021). Production of activated carbon from sawdust and its efficiency in the treatment of sewage water. *Heliyon, 7*(1), e05960. https://doi.org/10.1016/j.heliyon.2021.e05960

Omitola, O. B., Abonyi, M. N., Akpomie, K. G., & Dawodu, F. A. (2022). Adams-Bohart, Yoon-Nelson, and Thomas modeling of the fix-bed continuous column adsorption of amoxicillin onto silver nanoparticle-maize leaf composite. *Applied Water Science*, *12*(5). https://doi.org/10.1007/s13201-022-01624-4

Patel, H. (2019). Fixed-bed column adsorption study: a comprehensive review. In *Applied Water Science* (Vol. 9, Issue 3). Springer Verlag. https://doi.org/10.1007/s13201-019-0927-7

Pradeep, G. G., Sukumaran, K. P., George, G., Muhammad, F., & Mathew, N. (2016). PRODUCTION AND CHARACTERIZATION OF ACTIVATED CARBON AND ITS APPLICATION IN WATER PURIFICATION. *International Research Journal of Engineering and Technology*. www.irjet.net

Rathi, B. S., & Kumar, P. S. (2021). Application of adsorption process for effective removal of emerging contaminants from water and wastewater. Environmental Pollution, 280, 116995. https://doi.org/10.1016/j.envpol.2021.116995

Samarghandi, M. R., Dargahi, A., Shabanloo, A., Nasab, H. Z., Vaziri, Y., & Ansari, A. (2020). Electrochemical degradation of methylene blue dye using a graphite doped PbO2 anode: Optimization of operational parameters, degradation pathway and improving the biodegradability of textile wastewater. *Arabian Journal of Chemistry*, *13*(8), 6847–6864. https://doi.org/10.1016/j.arabjc.2020.06.038

Satyam, S., & Patra, S. (2024). Innovations and challenges in adsorption-based wastewater remediation: A comprehensive review. *Heliyon*, *10*(9). https://doi.org/10.1016/j.heliyon.2024.e29573

Sizirici, B., & Yildiz, I. (2020). Simultaneous removal of organics and metals in fixed bed using gravel and iron oxide coated gravel. *Results in Engineering*, *5*. https://doi.org/10.1016/j.rineng.2019.100093

So, S. H., & Oh, H. (2024). A mini-review of the current progress and future challenges of zeolites for hydrogen isotopes separation through a quantum effect. International Journal of Hydrogen Energy, 50, 539–560. https://doi.org/10.1016/j.ijhydene.2023.08.241

Tebeje, A., Worku, Z., Nkambule, T. T. I., & Fito, J. (2022). Adsorption of chemical oxygen demand from textile industrial wastewater through locally prepared bentonite adsorbent. *International Journal of Environmental Science and Technology*, 19(3), 1893–1906. https://doi.org/10.1007/s13762-021-03230-4

Wang, J., & Guo, X. (2020). Adsorption isotherm models: Classification, physical meaning, application and solving method. Chemosphere, 258, 127279. https://doi.org/10.1016/j.chemosphere.2020.127279

Yagub, M. T., Sen, T. K., Afroze, S., & Ang, H. M. (2014). Dye and its removal from aqueous solution by adsorption: A review. Advances in Colloid and Interface Science, 209, 172–184.